XLVI CILAMCE
VITÓRIA - ES - BRAZIL - 2025
XLVI IBERO-LATIN AMERICAN CONGRESS ON COMPUTATIONAL METHODS IN ENGINEERING

Numerical uncertainty quantification of the hemodynamic parameters of a cerebral aneurysm using the Grid Convergence Index (GCI) method

Gabriel Fávaro Pereira[1], Iago Lessa de Oliveira[2], Carlos Eduardo Baccin[3], José Luiz Gasche[1]

[1]*Dept. of Mechanical Engineering, São Paulo State University (Unesp)*
Avenida Brasil 56, 15385-007, Ilha Solteira, São Paulo, Brazil
gabriel-favaro.pereira@unesp.br, jose.gasche@unesp.br
[2]*Dept. of Mechanical Engineering, São Paulo State University (Unesp)*
Av. Eng. Luís Edmundo Carrijo Coube 14-01, 17033-360, Bauru, São Paulo, Brazil
iago.oliveira@unesp.br
[3]*Interventional Neuroradiologist, Albert Einstein Israelite Hospital*
Av. Albert Einstein, 627, 05652-900, São Paulo, São Paulo, Brazil
cebaccin@gmail.com

Abstract. A cerebral aneurysm consists of a pathological dilation of an intracranial artery, and its rupture is associated with a lethality rate of up to 50%. Computational Fluid Dynamics (CFD) has been widely used to investigate rupture risk factors by analyzing hemodynamic parameters of blood flow, especially the wall shear stress (WSS) and its time variation, quantified by the oscillatory shear index (OSI). A critical aspect of employing CFD is carefully managing discretization errors intrinsic to the computational mesh. Quantifying these errors and ensuring reliable results necessitates mesh convergence verification, which evaluates the solution's sensitivity to mesh refinement. A major challenge in CFD simulations of aneurysms is finding a mesh refinement level that balances result accuracy with computational cost. While most literature on the topic includes mesh refinement analysis, the uncertainty of numerical results, crucial for proper results interpretation, is rarely reported. A widely used approach in the literature to estimate discretization error and numerical uncertainty is the Grid Convergence Index (GCI). This study applies the GCI methodology to quantify numerical uncertainty from discretization in aneurysm blood flow simulations. The flow was solved using the Finite Volume Method implemented in the free, open-source software package OpenFOAM (Open Source Field Operation and Manipulation). We evaluated uncertainty by using three meshes generated with the OpenFOAM package. Numerical uncertainty was estimated for average WSS and OSI on the aneurysm sac surface to assess the rupture risk of a patient-specific aneurysm.

Keywords: Cerebral aneurysm, Computational fluid dynamics (CFD), Grid Convergence Index (GCI), Numerical uncertainty.

1 Introduction

Cerebral aneurysm is an abnormal dilation of an artery in the brain, resulting from a weakness in the vessel wall. Its most serious complication is rupture, which leads to blood leakage into the subarachnoid space—the region between the brain and its surrounding membranes—causing subarachnoid hemorrhage [1]. Studies indicate that hemodynamics plays a fundamental role in the formation, growth, and rupture of intracranial aneurysms [2].

In this context, Computational Fluid Dynamics (CFD) has been widely employed to investigate blood flow behavior in aneurysms based on three-dimensional reconstructions obtained from medical imaging [3]. Through this technique, it is possible to estimate relevant hemodynamic parameters such as wall shear stress (WSS) and the oscillatory shear index (OSI), which characterize the mechanical environment to which the aneurysm wall is subjected [4].

The accuracy of these results, however, strongly depends on the quality of the computational mesh. To reduce numerical discretization errors, it is essential to verify mesh convergence, ensuring that the solution is independent of the level of refinement used [5, 6]. Only a few studies have thoroughly assessed mesh and time-step induced errors in CFD simulations of arteries with cerebral aneurysms. Thus, the clinical use of CFD still faces resistance, particularly due to the lack of attention to the quantification of numerical uncertainties, which undermines the reliability of its results in medical applications [6]. Without a rigorous estimate of error margins, it becomes risky to use these simulations for diagnostic or prognostic purposes.

To address this challenge, methods for evaluating numerical uncertainty have become increasingly necessary in CFD studies applied to aneurysms. The Grid Convergence Index (GCI) method, recommended by the American Society of Mechanical Engineers (ASME), has been widely used in simulations of abdominal aortic aneurysms (AAA) to verify mesh independence. Aycan et al. [7], for example, analyzed the impact of different meshing strategies on the WSS distribution in patient-specific geometries. Similarly, Hodis et al. [6] demonstrated that variations in mesh refinement significantly affect parameters such as WSS, velocity, and pressure in five cases of cerebral aneurysms.

Therefore, the application of the GCI not only contributes to the reliability of the results but also strengthens the clinical validity of CFD-based studies. Thus, the objective of this work is to quantify the numerical uncertainty associated with mesh discretization in blood flow simulations of cerebral aneurysms using the GCI methodology. Three meshes with different refinement levels were analyzed, and the uncertainty was evaluated for the hemodynamic parameters WSS and OSI, both of which are relevant for assessing rupture risk.

2 Methodology

2.1 Geometry and Blood Flow Modeling

We used the geometry of a patient-specific internal carotid artery (ICA) harbouring a bifurcation aneurysm (see Fig. 1). The computational model was clipped at one inlet and three outlets.

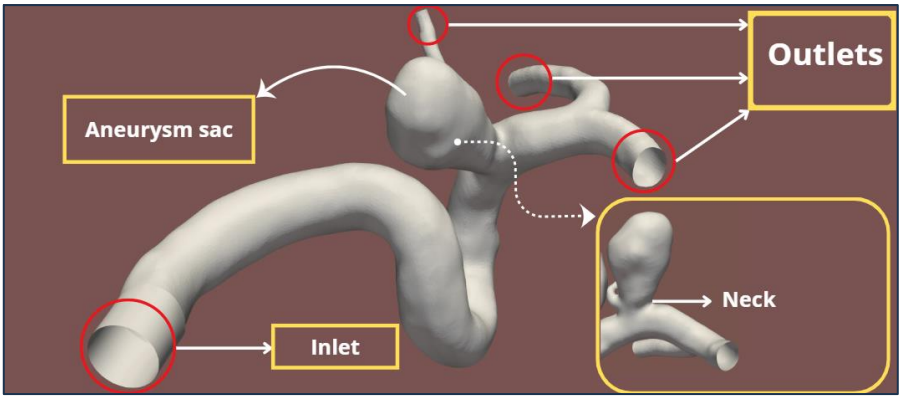


Figure 1. Aneurysm geometry used in this study, illustrating the main flow pathways through the vascular structure with one inlet, three outlets, the neck region, and the aneurysmal sac.

The three-dimensional model was generated from digital subtraction angiography (DSA) de-identified images provided by Dr. Carlos Eduardo Baccin in collaboration with Albert Einstein Israelita Hospital active scientific project. The VMTK® (Vascular Modeling Toolkit) software was used to segment the vascular surfaces and export the geometry in stereolithography (STL) format, which is compatible with CFD simulations.

The flow was considered incompressible, transient, and isothermal, appropriately representing blood flow in arteries. Thus, the governing equations for the flow are the continuity equation and the Navier–Stokes equations, respectively:

$$\nabla \cdot \vec{V} = 0 \tag{1}$$

$$\rho\left[\frac{\partial \vec{V}}{\partial t} + (\vec{V}\cdot\nabla)\vec{V}\right] = -\nabla p + \rho\vec{g} + \mu\nabla^2\vec{V} \tag{2}$$

where $\vec{V}$ is the velocity vector, ρ is the density, $\vec{g}$ is the gravitational acceleration vector, p is the pressure, and μ is the dynamic viscosity. In this study, the dynamic viscosity of blood was assumed to be $\mu = 3.5 \times 10^{-3}$ Pa · s.

The boundary conditions were defined based on physiological data characteristic of cerebral circulation, in order to ensure a realistic representation of the flow. The conditions applied in the simulation are described below:

- **Inlet**: At the domain inlet, a time-varying volumetric flow rate $\bar{q}_a(t)$ (Fig. 2) was imposed, representing the pulsatile pattern of the cardiac cycle. This flow rate was derived from the normalized volumetric flow rate (VVN), as proposed by Ford et al. [8], multiplied by the mean volumetric flow rate in the internal carotid artery (VVM), which was obtained from a sample of older adult patients and reported by Zarrinkoob et al. [9] as 4.3 mL/s, according to the equation:

$$q_a = VVM * VVN \tag{3}$$

This approach was adopted due to the absence of patient-specific flow data, allowing for a physiologically inlet flow representation. A zero-gradient condition was applied for pressure at the inlet.

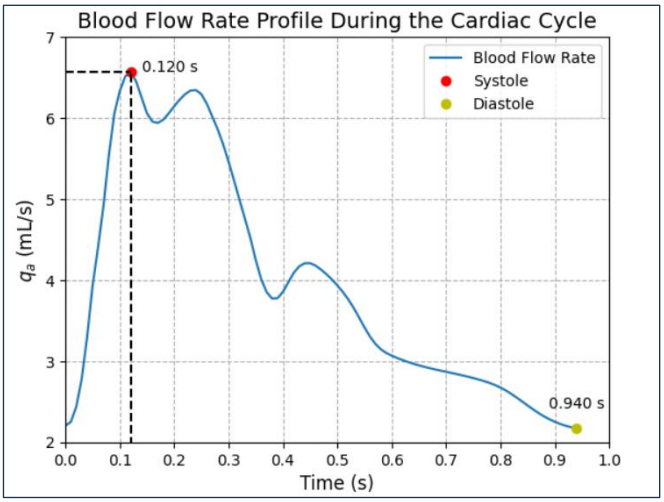


Figure 2. Temporal profile of volumetric flow rate in the main vertebral artery.

- **Outlets**: At the outlets, a boundary condition that adjusts the velocity based on the flow and the orientation of the outlet face (*fluxCorrectedVelocity*):

$$U_p = U_c - n(n\cdot U_c) + \frac{n\varphi_p}{|S_f|} \tag{4}$$

where U_p is the velocity at the outlet patch (m/s), U_c is the velocity in the cells adjacent to the patch (m/s), n is the normal vector to the outlet patch, φ_p is the flux at the patch (m³/s), and S_f is the area of the outlet patch (m²). The outlet pressure was prescribed based on a value proportional to the inlet flow rate [10].

- **Wall**: The vessel walls were considered rigid and impermeable, neglecting elastic deformations during the cardiac cycle. No-slip conditions were applied, i.e., zero velocity at the fluid–wall interface, and a zero-gradient condition was imposed for pressure in the directions normal to the wall.

2.2 Computational Mesh and Numerical Strategies

Equations (1) and (2), along with the boundary conditions, were discretized using the Finite Volume Method, implemented in OpenFOAM®. The pisoFoam solver was employed, which is suitable for incompressible and transient flows due to its use of the PISO (Pressure Implicit with Splitting of Operators) algorithm, providing stability and efficiency in solving the pressure–velocity coupling [11].

The mesh generation was carried out in two stages. Initially, the blockMesh tool was used to create a primitive structured mesh composed of regular hexahedral volumes. Subsequently, the snappyHexMesh tool was employed to adapt the mesh to the three-dimensional aneurysm geometry, performing local refinements and gradually adjusting the cells to the vascular surface. Figure 3 presents a visualization of the final mesh, showing the refinement and good conformity to the aneurysm surface.

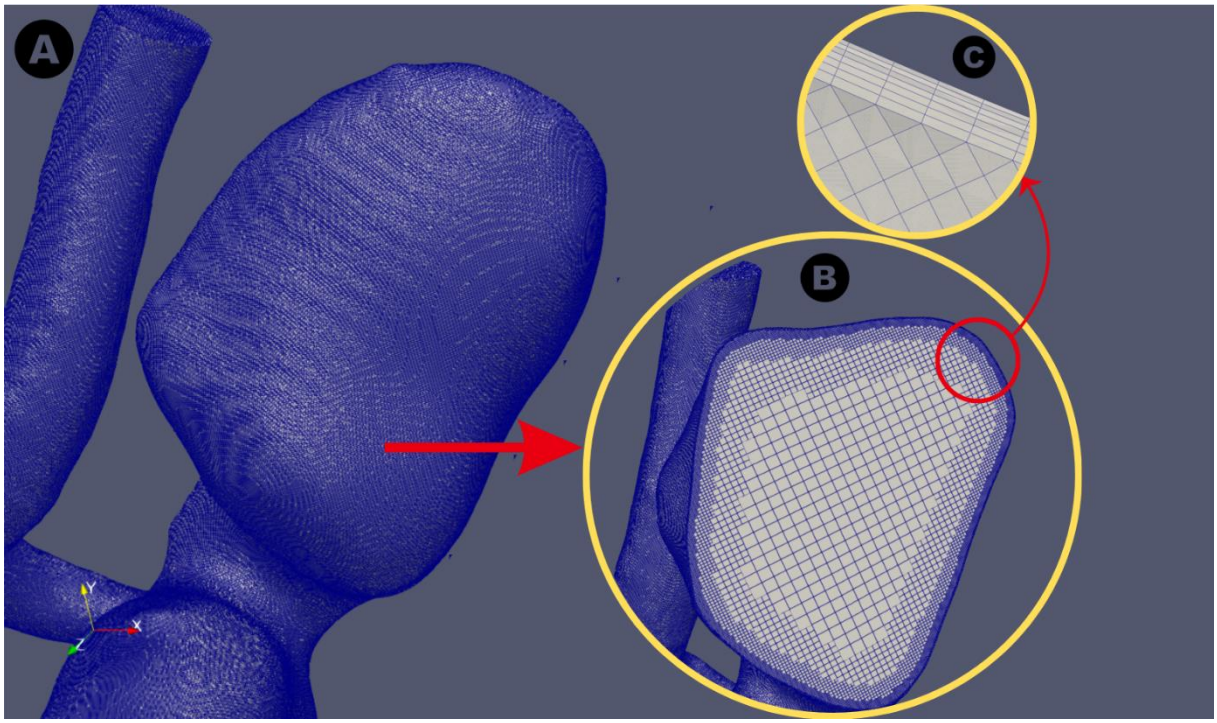


Figure 3. Computational mesh generated after applying *snappyHexMesh*, showing: (a) external mesh; (b) internal mesh, highlighting the refinement levels up to the aneurysm wall; and (c) refinement layer near the wall.

The mesh quality was assessed using the metrics aspect ratio, non-orthogonality, and skewness. All metrics met the minimum criteria recommended by OpenFOAM®, with non-orthogonality values below 69° and a maximum skewness of 6.8 — above the recommended limit of 4. Although some cells exhibited distortions beyond the ideal range, this is common in complex geometries and did not compromise mesh quality for the case under study.

Three meshes with increasing levels of refinement were generated to evaluate mesh independence and the associated numerical uncertainty: coarse (3.95 million cells), medium (6.84 million cells), and fine (11.69 million cells).

2.3 Calculation of Hemodynamic Parameters

Three of the main hemodynamic parameters related to the wall shear stress field (WSS) were calculated: TAWSS (Time-Averaged Wall Shear Stress), OSI (Oscillatory Shear Index), and PSWSS (Peak-Systole Wall Shear Stress). These parameters are widely used in the literature as they capture different aspects of blood flow over the vascular wall.

TAWSS is defined as the time-averaged magnitude of WSS and is calculated by the following equation:

$$TAWSS(x) \equiv \overline{\tau_w}(x) = \frac{1}{T_c}\int_0^{T_c} \|\boldsymbol{\tau_w}\| \, dt \tag{5}$$

where T_c is the duration of the cardiac cycle, and $\boldsymbol{\tau_w}$ is the wall shear stress vector. The integral in the numerator sums the magnitude of WSS at each moment of the cycle, while the division by T_c normalizes this sum, yielding the time average. This metric allows the identification of arterial wall regions subjected to high or low shear levels,

which are important for analyzing vascular dynamics.

The OSI quantifies the variation in the direction of the wall shear stress vector throughout the cardiac cycle, characterizing the directionality of near-wall blood flow. It is given by:

$$OSI(x) = \frac{1}{2}\left(1 - \frac{\left\| \frac{1}{Tc}\int_0^{T_c} \boldsymbol{\tau_w}\, dt \right\|}{\frac{1}{T_c}\int_0^{T_c} \|\boldsymbol{\tau_w}\|\, dt}\right) \tag{6}$$

In this equation, the numerator represents the time-averaged WSS vector considering its direction, while the denominator is the average of the WSS magnitude, regardless of direction.

Finally, the PSWSS parameter was defined as the wall shear stress (WSS) at the peak-systole instant during the cardiac cycle (see Fig. 2).

These parameters were obtained from the transient results of the numerical simulations, considering the periodic behavior of blood flow in the cerebral aneurysm over the cardiac cycle, using the vmtk4aneurysms library [12].

2.4 Numerical Convergence Analysis via the GCI Method

The numerical convergence analysis followed the GCI method (Grid Convergence Index), as recommended by Celik et al. [13] and by the guidelines of the *ASME Journal of Fluids Engineering* (2008), with the aim of estimating discretization error and verifying the independence of results with respect to mesh resolution.

After running simulations with three meshes of different refinement levels, the GCI analysis was carried out in six steps:

Step 1: A representative mesh size, h, suitable for three-dimensional calculations, was defined and computed according to eq. (7):

$$h = \left(\frac{1}{N}\sum_{i=1}^{N} \Delta V_i\right)^{\frac{1}{3}} \tag{7}$$

where N is the total number of elements and ΔV_i is the volume of the i-th control volume.

Step 2: The refinement ratio (r) was calculated using eq. (8), for each pair of consecutive meshes—coarse to medium and medium to fine:

$$r = \frac{h_{\text{coarse}}}{h_{\text{fine}}} > 1{,}3 \tag{8}$$

Step 3: The meshes were grouped into two pairs (mesh 1 and mesh 2; mesh 2 and mesh 3), and the apparent order of accuracy p was calculated using the equations below:

$$p = \frac{1}{\ln(r_{21})}\left| \ln\left|\frac{\varepsilon_{32}}{\varepsilon_{21}}\right| + q(p) \right| \tag{9}$$

$$q(p) = \ln\left(\frac{r_{21}^p - s}{r_{32}^p - s}\right) \tag{10}$$

where $s = \text{sgn}\,(\varepsilon_{32}/\varepsilon_{21})$, $\varepsilon_{21} = \phi_2 - \phi_1$ and $\varepsilon_{32} = \phi_3 - \phi_2$, with ϕ_1, ϕ_2, and ϕ_3 representing the values of the variable of interest—namely the hemodynamic parameters—obtained respectively from the fine, medium, and coarse meshes. A negative value of $\varepsilon_{32}/\varepsilon_{21}$ indicates oscillatory convergence.

Step 4: The extrapolated values of ϕ were computed using eq. (11):

$$\phi_{\text{ext},32} = \frac{r_{32}^p \phi_3 - \phi_2}{r_{32}^p - 1} \quad ; \quad \phi_{\text{ext},21} = \frac{r_{21}^p \phi_1 - \phi_2}{r_{21}^p - 1} \tag{11}$$

Step 5: The approximate relative errors and the extrapolated relative errors were estimated by:

$$\varepsilon_{a,32} = \left|\frac{\phi_2 - \phi_3}{\phi_2}\right| \quad ; \quad \varepsilon_{a,21} = \left|\frac{\phi_1 - \phi_2}{\phi_1}\right| ; \quad \varepsilon_{\text{ext},32} = \left|\frac{\phi_{\text{ext},23} - \phi_2}{\phi_{\text{ext},23}}\right| \quad ; \quad \varepsilon_{\text{ext},21} = \left|\frac{\phi_{\text{ext},12} - \phi_1}{\phi_{\text{ext},12}}\right| \tag{12}$$

Step 6: Finally, the GCI for each pair of meshes was calculated as:

$$\mathrm{GCI}_{\mathrm{fine},32} = 1{,}25 \cdot \frac{\varepsilon_{a,32}}{r_{32}^{p} - 1} \quad ; \quad \mathrm{GCI}_{\mathrm{fine},21} = 1{,}25 \cdot \frac{\varepsilon_{a,21}}{r_{21}^{p} - 1} \tag{13}$$

where Fs = 1,25 corresponds to the safety factor recommended by ASME for convergence studies using three mesh levels.

3 Results and discussion

The convergence analysis aimed to ensure the independence of the results with respect to the mesh and to quantify the numerical uncertainty of the hemodynamic variables analyzed. The characteristics of the meshes used are presented in Tab. 1.

Table 1. Selected mesh set.

Mesh	Representative cell size h [mm]	Number of cells N	Refinement ratio (r)
1	$5{,}302\times10^{-5}$	11691002	-
2	$6{,}340\times10^{-5}$	6837098	$r_{21} = 1{,}1958$
3	$7{,}612\times10^{-5}$	3949208	$r_{32} = 1{,}2007$

From the three meshes, the values of the three hemodynamic variables of interest were extracted: OSI, TAWSS, and PSWSS. These values were used to estimate the apparent order of convergence and the associated discretization error. Table 2 summarizes the main parameters, including the convergence order (p) and the relative/extrapolated errors for the fine and coarse meshes.

Table 2. Relative and extrapolated errors.

Variable	Order (p)	$\varepsilon_{a,32}$ (%)	$\varepsilon_{a,21}$ (%)	$\varepsilon_{ext,32}$(%)	$\varepsilon_{ext,21}$(%)
OSI	8,121	2,4	0,53	0,7	0,16
TAWSS	7,305	0,05	0,18	0,02	0,07
PSWSS	2,362	0,56	0,36	1,05	0,69

Table 2 shows that the relative errors between adjacent meshes were low for all variables, especially for OSI and TAWSS. The observed convergence orders for TAWSS ($p \approx 7{,}31$) and OSI ($p \approx 8{,}12$) were significantly high. For PSWSS, although the convergence order was lower ($p \approx 2{,}36$), the relative errors remained within acceptable levels, with values below 1,1%.

Table 3 shows the GCI values for all variables. It is observed that GCI values were below 1% for all variables. TAWSS showed the lowest GCI values, below 0,1% in both mesh pairs (32 and 21), indicating excellent reliability and mesh independence. For OSI, GCI values remained below 1%, demonstrating good numerical stability and low sensitivity to refinement. Although PSWSS presented the highest GCI values, up to 1,30%, they are still within acceptable limits for CFD simulations.

These results enable practical recommendations regarding mesh size and acceptable error levels. For example, Mesh 2 (intermediate resolution) showed GCI values below 1% for TAWSS and OSI, indicating that it may be sufficient for studies focused on these variables with moderate computational resources. However, in cases involving more sensitive parameters, such as PSWSS, or when higher numerical accuracy is required, the use of Mesh 1 (more refined) is recommended, as it ensures errors below 1% for all evaluated quantities.

Therefore, for similar CFD studies of intracranial aneurysms, using a mesh with an average cell size below $6{,}340\times10^{-5}$ mm (as in Mesh 2) appears sufficient to ensure errors below 1% for most hemodynamic parameters. However, when aiming for high-fidelity analysis involving parameters such as PSWSS, finer meshes like Mesh 1 should be prioritized, even with higher computational costs.

Table 3. Grid Convergence Index Analysis.

Variable	$GCIfine_{32}$ (%)	$GCIfine_{21}$ (%)
OSI	0,88	0,2
TAWSS	0,02	0,08
PSWSS	1,3	0,86

4 Conclusions

The results of this study demonstrate that, although the numerical uncertainties associated with mesh discretization are low (GCI < 1.3% for all analyzed hemodynamic parameters), their quantification is essential to ensure the reliability of CFD simulations in cerebral aneurysms. In clinical applications, even small variations in WSS or OSI values can influence the assessment of rupture risk and, consequently, clinical decision-making.

Thus, the application of the GCI method contributes not only to validating the robustness of the numerical models but also to increasing confidence in the use of the results in clinical contexts. The adoption of verification procedures, as carried out in this study, is fundamental for computational simulations to accurately and safely support diagnosis and treatment planning.

Acknowledgements. G. F. Pereira gratefully acknowledges the financial support from Coordenação de Aperfeiçoamento de Pessoal de Nível Superior – Brasil (CAPES) – Finance Code 001.

Authorship statement. The authors hereby confirm that they are the sole liable persons responsible for the authorship of this work.

References

[1] T. L. Rolim Júnior and A. C. C. M. Guimarães. Aneurisma cerebral: manifestações clínicas e conduta cirúrgica. *Revista Ibero-Americana de Humanidades, Ciências e Educação*, vol. 9, n. 9, pp. 3239–3249, 2023.
[2] H. Meng et al. High WSS or low WSS? Complex interactions of hemodynamics with intracranial aneurysm initiation, growth, and rupture: toward a unifying hypothesis. *AJNR. American Journal of Neuroradiology*, vol. 35, n. 7, pp. 1254-1262, 2014.
[3] M. R. Levitt et al. Computational fluid dynamics of cerebral aneurysm coiling using high resolution and high-energy synchrotron X-ray microtomography: comparison with the homogeneous porous medium approach. *Journal of Neurointerventional Surgery*, vol. 9, n. 8, 2017.
[4] C. Sherif et al. Computational fluid dynamic simulations of cerebral aneurysms. *Advances in Experimental Medicine and Biology*, vol. 1462, pp. 397-415, 2024.
[5] M. O. Khan, K. Valen-Sendstad, and D. A. Steinman. Narrowing the expertise gap for predicting intracranial aneurysm hemodynamics: Impact of solver numerics versus mesh and time-step resolution. *American Journal of Neuroradiology*, vol. 36, n. 7, pp. 1310–1316, 2015.
[6] S. Hodis et al. Grid convergence errors in hemodynamic solution of patient-specific cerebral aneurysms. *Journal of Biomechanics*, vol. 45, pp. 2907-2913, 2012.
[7] O. Aycan, A. Topuz, and L. Kadem. Evaluating uncertainties in CFD simulations of patient-specific aorta models using Grid Convergence Index method. *Mechanics Research Communications*, vol. 133, 2023.
[8] M. D. Ford et al. Characterization of volumetric flow rate waveforms in the normal internal carotid and vertebral arteries. *Physiological Measurement*, vol. 26, n. 4, pp. 477-488, 2005.
[9] L. Zarrinkoob et al. Blood flow distribution in cerebral arteries. *Journal of Cerebral Blood Flow and Metabolism*, vol. 35, no. 4, pp. 648-654, 2015.
[10] C. Chnafa, O. Brina, V. M. Pereira, and D. A. Steinman. Better than nothing: a rational approach for minimizing the impact of outflow strategy on cerebrovascular simulations. *AJNR. American Journal of Neuroradiology*, vol. 39, n. 2, pp. 337–343, 2018.
[11] G. D. M. Cambeell. Evaluación de los efectos de flujo cavitativo en estrangulamiento aplicado a válvulas hidráulicas. Dissertação (Mestrado em Física aplicada) – Facultad de Ingeniería en sistemas, electrónica e industrial, Universidad Técnica de Ambato, Ambato/EC, 2022.
[12] I. Lessa. vmtk4aneurysms: Release version 1.0.0. Zenodo, 2022. doi: 10.5281/zenodo.6675879.
[13] I. B. Celik et al. Procedure for estimation and reporting of uncertainty due to discretization in CFD applications. *ASME, Journal of Fluids Engineering*, vol. 130, n. 7, 2008.